Eur Biophys J (2009) 38:547–556
DOI 10.1007/s00249-009-0403-7

ORIGINAL PAPER

Study of kinetics of thermal aggregation of mitochondrial aspartate aminotransferase by dynamic light scattering: protective effect of α-crystallin

Nikolay V. Golub · Kira A. Markossian · Mikhail V. Sholukh · Konstantin O. Muranov · Boris I. Kurganov

Received: 3 July 2008 / Revised: 18 November 2008 / Accepted: 2 January 2009 / Published online: 27 January 2009

Abstract Thermal aggregation of aspartate aminotransferase from pig heart mitochondria (mAAT) has been studied at various temperatures and various protein concentrations by dynamic light scattering. The character of the dependence of protein aggregate size on time indicates that aggregation of mAAT proceeds in the regime of diffusion-limited cluster–cluster aggregation. Suppression of mAAT aggregation by α-crystallin is due to transition of the aggregation process into the regime of reaction-limited cluster–cluster aggregation. Realization of this regime of aggregation means that the sticking probability for the colliding particles is less than unity.

Keywords Mitochondrial aspartate aminotransferase · Aggregation · α-Crystallin · Dynamic light scattering

Introduction

Protein aggregation accompanied by formation of insoluble intracellular complexes and inclusion bodies is a problem, which is associated with biotechnological tasks and underlies pathogenesis of many human degenerative and neurodegenerative diseases (Jaenicke 1995; Fink 1998; Dobson 1999; Markossian and Kurganov 2004). Because of the low conformational stability of the protein native state, relatively small changes in external conditions (temperature, pH, salt addition) may destabilize the structure of the protein and induce its unfolding and aggregation. Aggregates are produced when unfolded proteins interact mainly through contact of their hydrophobic surfaces (Jaenicke 1998; Fink 1998; Dobson 1999; Kopito 2000; Markossian and Kurganov 2004).

Proteins exhibit some of the physical chemical properties of colloids, and physical laws derived for the formation and aggregation of colloids can be applied to protein aggregation (Xu et al. 2005). Two distinct limiting regimes of irreversible colloid aggregation have been identified: diffusion-limited cluster–cluster aggregation (DLCA) and reaction-limited cluster–cluster aggregation (RLCA) (Weitz et al. 1984, 1985; Ball et al. 1987; Lin et al. 1989). DLCA occurs when there is no repulsive force between colloidal particles and the aggregation rate is only dependent on the time for particles (or clusters) to collide by diffusion. In the DLCA regime a rigid bond is formed at each collision of particles. The clusters continue to diffuse, collide and form larger clusters. Analysis of kinetics of protein aggregation obtained by means of dynamic light scattering showed that in the DLCA regime, the dependence of the hydrodynamic radius R_h on time follows the power law. In the RLCA regime, additional repulsive forces caused by electrostatic forces prevent the particles from coagulating and the bond formation probability decreases to zero. In this case, the dependence of the hydrodynamic radius on time follows the exponential law (Weitz et al. 1985; Lin et al. 1989). It has been shown that each of these limiting regimes is associated with characteristic cluster growth kinetics and a cluster morphology that is

N. V. Golub · K. A. Markossian · B. I. Kurganov (✉)
Bach Institute of Biochemistry, Russian Academy of Sciences, Moscow, Russia
e-mail: kurganov@inbi.ras.ru

M. V. Sholukh
Belarusian State University, Minsk, Belarus

K. O. Muranov
Emanuel Institute of Biochemical Physics, Russian Academy of Sciences, Moscow, Russia

independent of the chemical properties of a particular colloid system (Lin et al. 1989).

Irreversible aggregation leads to the formation of self-similar aggregates with a fractal dimension of 1.8 for the DLCA regime and 2.1 for the RLCA regime. A scaling analysis of light scattering data used to compare aggregation behavior provided convincing experimental evidence that the two aggregation regimes are universal (Ball et al. 1987; Berka and Rice 2005).

The approaches developed to study aggregation of colloid particles have been used for the analysis of kinetics of thermal aggregation of proteins (Nicolai et al. 1994; Andreasi Bassi et al. 1995; Le Bon et al. 1999; Pouzot et al. 2004). Thermal aggregation of proteins usually proceeds in the DLCA regime (Khanova et al. 2005; Markossian et al. 2006a; Panyukov et al. 2007; Meremyanin et al. 2008). When protein aggregation occurred in the presence of α-crystallin, the RLCA regime was observed (Khanova et al. 2005; Markossian et al. 2006b; Meremyanin et al. 2008).

α-Crystallin, a member of the small heat-shock protein (sHSP) superfamily, possesses chaperone-like activity and suppresses heat-induced aggregation and precipitation of many partially denatured proteins (Horwitz 1992; Wang and Spector 1994, Abgar et al. 2001; Putilina et al. 2003). In native state α-crystallin is a heterogeneous oligomer composed of two kinds of subunits, αA- and αB-crystallin, each of molecular weight of about 20 kDa (Groenen et al. 1994; Horwitz 2003). A dynamic quaternary structure of α-crystallin depends on external conditions such as pH, temperature, ionic strength and concentration, and the number of subunits in each assemblage can vary from 15 to 50 (Vanhoudt et al. 1997; Burgio et al. 2000). The ability of α-crystallin to suppress heat-induced aggregation of proteins is a result of its complexation with denatured proteins as demonstrated by different physical and physico-chemical methods (Horwitz 1993; Wang and Spector 1994; Putilina et al. 2003; Krivandin et al. 2004). It is of special interest to clear up whether the protective mechanism of α-crystallin proposed by us (Khanova et al. 2005; Markossian et al. 2006b; Meremyanin et al. 2008) and based on the transition of the aggregation process from the DLCA regime to RLCA regime is universal.

In some cases the RLCA regime for protein aggregation can be realized in the absence of an added chaperone. Such a situation is observed when the protein contains an intramolecular chaperone. When analyzing the kinetics of thermal aggregation of yeast alcohol dehydrogenase I, we showed that the initial parts of the dependences of the hydrodynamic radius on time follow the exponential law (Markossian et al. 2008). According to (Bhattacharyya et al. (2003), the peptide -SGVCHTDLHAWHGDWPL PVK [40–60]- of the alcohol dehydrogenase I molecule functions as an intramolecular chaperone. Thus, analysis of the dependence of the hydrodynamic radius of protein aggregates on time permits to reveal the proteins that contain intramolecular chaperones. When choosing protein substrates for testing chaperone-like activity, preference should be given to proteins with well-studied mechanism of denaturation and aggregation.

Aspartate aminotransferase (EC 2.6.1.1, mAAT) from pig heart mitochondria is a homodimeric, pyridoxal 5′-phosphate (PLP)-dependent enzyme, which contains one molecule of PLP bound to each of the two identical active sites (Boyd 1961). The molecular mass of dimeric mitochondrial enzyme is about 92.9 kDa (Barra et al. 1976). The functionally independent active sites are at the interface between the small and large domains on the opposite sides of the dimeric molecule (Ford et al. 1980). Inactivation and denaturation of mAAT have been in the focus of some studies (Twomey and Doonan 1997; Azzariti et al. 1998; Lawton and Doonan 1998; Golub et al. 2008). In our previous study we have shown that inactivation and denaturation of mAAT proceed as irreversible reactions of the first order (Golub et al. 2008).

In the present work we demonstrate that thermal aggregation of mAAT proceeds in the DLCA regime. The obtained results suggest that the protective action of α-crystallin is due to diminution in the size of the start aggregates and the transition of the aggregation process into the RLCA regime.

Materials and methods

Materials

All solutions for the experiments were prepared using deionized water obtained with Easy-Pure II RF system (Barnstead, USA).

Isolation and purification of mAAT

The enzyme was purified according to (Barra et al. (1976) with several modifications (Golub et al. 2008). Protein concentration was determined from the absorbance at 280 nm using the extinction coefficient $A_{280}^{1\%} = 14.0$ (Barra et al. 1976).

Isolation and purification of α-crystallin

Purification of α-crystallin from freshly excised lenses of 2-year-old steers was performed according to the procedure described earlier (Chiou et al. 1979; Khanova et al. 2005). The α-crystallin concentration was determined from the absorbance at 280 nm using the extinction coefficient $A_{280}^{1\%}$ = of 8.5 (Putilina et al. 2003).

Dynamic light scattering (DLS) studies

For light scattering measurements a commercial instrument Photocor Complex was used (Photocor Instruments Inc., USA; www.photocor.com) with an He–Ne laser (Coherent, USA, Model 31–2082, 632.8 nm, 10 mW) as a light source. The temperature of sample cell was controlled by the proportional integral derivative (PID) temperature controller to within ±0.1°C. A quasi-cross correlation photon counting system with two photomultiplier tubes (PMT) was used to increase the accuracy of particle sizing in the range from 1.0 nm to 5.0 μm. DLS data were accumulated and analyzed with multifunctional real-time correlator Photocor-FC. DynaLS software (Alango, Israel) was used for polydisperse analysis of DLS data.

The diffusion coefficient D of the particles is directly related to the decay rate τ_c of the time-dependent correlation function for the light-scattering intensity fluctuations: $D = 1/2\tau_c k^2$. In this equation k is the wave number of the scattered light, $k = (4\pi n/\lambda)\sin(\theta/2)$, where n is the refractive index of the solvent, λ is the wavelength of the incident light in vacuum and θ is the scattering angle. The mean hydrodynamic radius of the particles, R_h, can then be calculated according to the Stokes–Einstein equation: $D = k_B T/6\pi\eta R_h$, where k_B is Boltzmann's constant, T is the absolute temperature and η is the shear viscosity of the solvent.

Thermal aggregation of mAAT was studied in 10 mM Na-phosphate buffer, pH 7.5. The buffer was placed in a cylindrical cell with a diameter of 6.3 mm and pre-incubated for 10 min at appropriate temperature. Cells with stoppers were used for incubation at high temperature to avoid evaporation. The aggregation process was initiated by the addition of an aliquot of mAAT to a final volume of 0.5 ml. To study the effect of α-crystallin on aggregation of mAAT, aliquots of both proteins were added into the cell simultaneously. The scattering light was collected at 90° scattering angle and the accumulation time of the autocorrelation function was 30 s.

Analysis of the dependence of the hydrodynamic radius of the protein aggregates on time allows discriminating between the DLCA and RLCA regimes of aggregation. In our previous works (Khanova et al. 2005; Markossian et al. 2006a, 2006b; Panyukov et al. 2007), the conclusion about the validity of the DLCA regime was made on the fact that from a certain value of time ($t > t^*$) the dependence of the hydrodynamic radius (R_h) of the protein aggregates on time follows the power law (Khanova et al. 2005; Markossian et al. 2006a, 2006b; Panyukov et al. 2007):

$$R_h = R_h^*[1 + K_2(t - t^*)]^{1/d_f}, \quad (1)$$

where R_h^* is the R_h value at $t = t^*$, K_2 is a constant and d_f is the fractal dimension of the fractal aggregates. For the DLCA regime parameter d_f has a universal value: $d_f = 1.8$ (Lin et al. 1989; Weitz et al. 1984, 1985).

The initial parts of the dependences of hydrodynamic radius on time for protein aggregation proceeding in the DLCA regime are described by the linear function (Khanova et al. 2005; Markossian et al. 2006a, 2006b):

$$R_h = R_{h,0}(1 + t/t_{2R}), \quad (2)$$

where $R_{h,0}$ is the hydrodynamic radius of the start aggregates and t_{2R} is the time interval over which the $R_{h,0}$ value increases from $R_{h,0}$ to $2R_{h,0}$.

The linear character of the initial parts of the dependences of R_h on time observed by us for protein aggregation is not an extraordinary feature of colloid aggregation. When studying the kinetics of colloid aggregation proceeding in the DLCA regime, the dependences of R_h on time at rather low values of time are linear, as was clearly demonstrated, for example, for aggregation of kaolinite (Berka and Rice 2005).

The light scattering intensity (I) versus the hydrodynamic radius plots may be used for estimation of the size of the start aggregates. The $R_{h,0}$ value corresponds to the length cut off on the abscissa axis by the linear dependence of I on R_h (Khanova et al. 2005; Markossian et al. 2006a, 2006b). The dimensionless polydispersity index PI, which is a measure of the breadth of the distribution of particles by size, was calculated according to International standard ISO 13321 (International standard ISO 13321:1996(E) 1996).

Results and discussion

Kinetics of thermal aggregation of mAAT

Figure 1 shows the increase in the light scattering intensity at 632.8 nm accompanying thermal aggregation of mAAT at 55°C (a), 57.5°C (b) and 60°C (c) (10 mM Na-phosphate buffer, pH 7.5). The enhancement of the enzyme concentration in the interval from 0.05 to 0.4 mg/ml results in the increase in the increment rate of the light scattering intensity (curves 1–4 in Fig. 1a–c). At sufficiently high values of incubation time a decrease in the light scattering intensity occurs because of precipitation of the protein aggregates.

It is of interest that the ascending branches of the dependences of the light scattering intensity (I) on time (below the time value where precipitation is observed) for mAAT aggregation follow the exponential law (see Kurganov 2002a):

$$I = I_{lim}[1 - \exp(-k_I t)], \quad (3)$$

where I_{lim} is the limiting value of I at $t \to \infty$ and k_I is the rate constant of the first order The results of fitting are shown in Fig. 1.

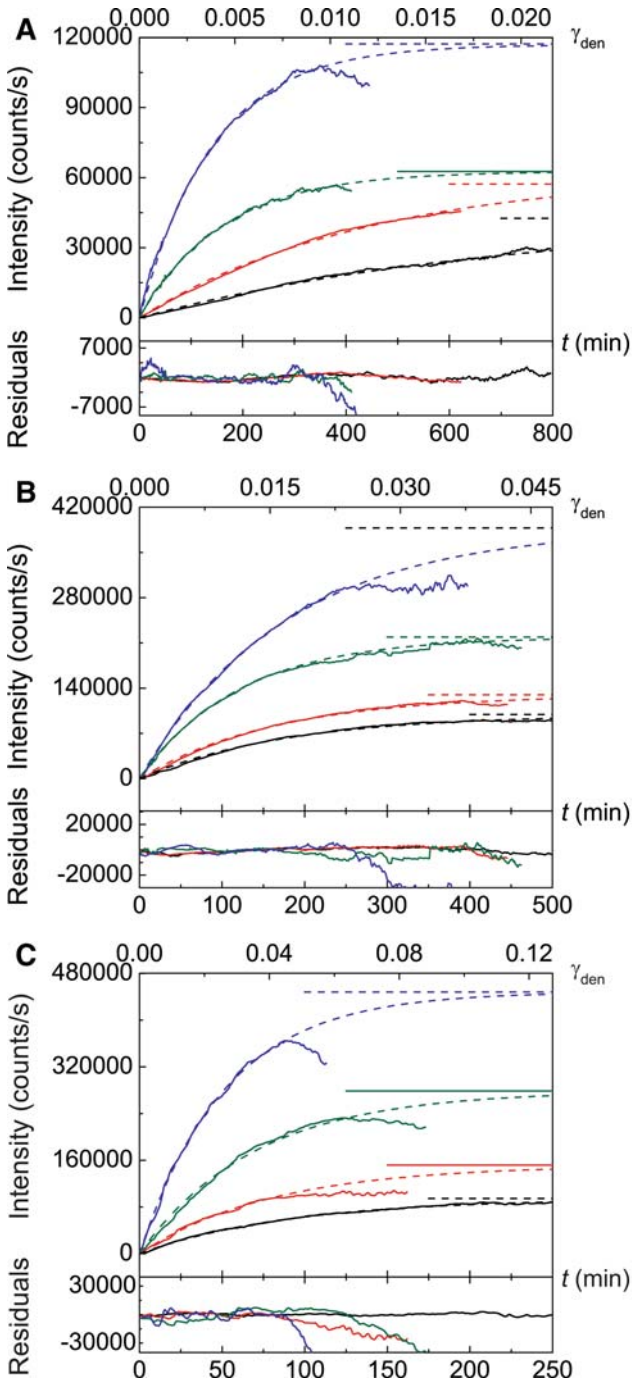

Fig. 1 Thermal aggregation of mAAT (10 mM Na-phosphate buffer, pH 7.5). Dependences of the light scattering intensity on time obtained at 55°C (**a**), 57.5°C (**b**) and 60°C (**c**). The protein concentrations were as follows: 0.05 (*1*), 0.1 (*2*), 0.2 (*3*) and 0.4 (*4*) mg/ml. The *dotted curves* are calculated from Eq. (3). The *horizontal dotted lines* correspond to the I_{lim} values. The *upper scales* in (**a**–**c**) show the portion of the denatured protein (γ_{den}) calculated from Eq. (4) with the values of k_{den} equal to 2.7×10^{-5}, 1.2×10^{-4} and 5.1×10^{-4} min^{-1} at 55, 57.5 and 60°C, respectively

At first glance, the course of the theoretical curve described by Eq. (3) corresponds to the aggregation process developing under the conditions of lacking precipitation. In this case the I_{lim} value would correspond to the complete transition of the protein to the aggregated form. However, the calculation of a portion of the denatured protein shows that in the time intervals under investigation the aggregation process is far from completion. Since the process of mAAT thermal aggregation proceeds as a monomolecular irreversible reaction (Golub et al. 2008), the portion of denatured protein may be calculated as follows: $\gamma_{den} = 1 - \exp(-k_{den}t)$, where k_{den} is the denaturation rate constant. To calculate the k_{den} values at various temperatures, we used the Arrhenius equation in the following form:

$$k_{den} = \exp\left\{\frac{E_a^{den}}{R}\left(\frac{1}{T_1^{den}} - \frac{1}{T}\right)\right\} min^{-1}, \quad (4)$$

where E_a^{den} is the energy of activation, T_1^{den} is the temperature at which the rate constant k_{den} equals 1 min^{-1} and R is the gas constant. The values of parameters E_a^{den} and T_1^{den} were found to be 516.6 ± 0.7 kJ mol^{-1} and 346.44 ± 0.01 K, respectively (10 mM Na-phosphate buffer, 7.5) (Golub et al. 2008). The values of k_{den} at 55°C (a), 57.5°C (a) and 60°C (c) calculated from Eq. (4) were equal to 2.7×10^{-5}, 1.2×10^{-4} and 5.1×10^{-4} min^{-1}, respectively. The upper scales in Fig. 1a–c show the increase in the portion of the denatured protein (γ_{den}) in the course of mAAT denaturation at the corresponding temperatures. Previously we showed that the portion of the aggregated protein (γ_{agg}) determined in the sedimentation experiments coincided with the portion of the denatured protein (Golub et al. 2008). To characterize the time of the leveling off of the light scattering intensity, parameter $t_{0.99}$ may be used by convention: $t_{0.99}$ is the time value at which the light scattering intensity reaches the level of $I/I_\infty = 0.99$. The values of $t_{0.99}$ for the theoretical dependences of the light scattering intensity on time calculated from Eq. (3) at 55°C (a), 57.5°C (b) and 60°C (c) at mAAT concentration of 0.05 mg/ml were equal to 3,270, 820 and 490 min, respectively. These $t_{0.99}$ values correspond to the following values of $\gamma_{den} = \gamma_{agg}$: 0.08, 0.09 and 0.22. The analogous calculations were made for other concentrations of mAAT. The leveling off of the light scattering intensity takes place at time values when the portion of the denatured protein does not exceed 22% (under the studied conditions).

Measurements of the hydrodynamic radius of the protein aggregates formed at thermal aggregation of mAAT have allowed us to explain why precipitation of mAAT aggregates proceeds at low values of protein denaturation. Treatment of the DLS data shows that the distribution of protein aggregates by size in the course of thermal aggregation of mAAT remains unimodal, with the position of the distribution peak shifted to higher values of the hydrodynamic radius when the incubation time rises. Figure 2

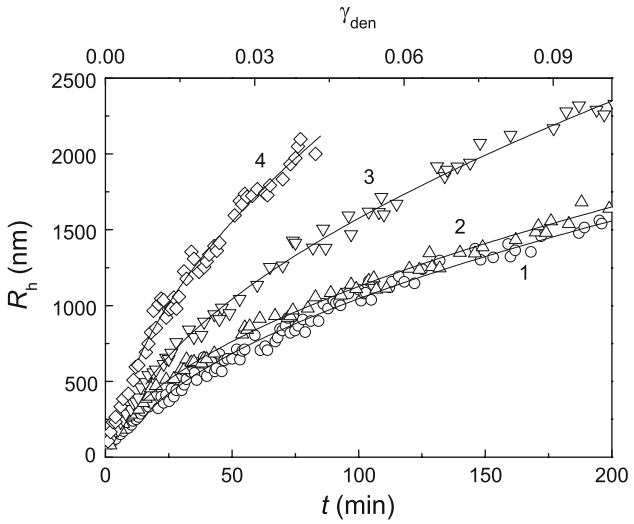

Fig. 2 Dependences of the hydrodynamic radius (R_h) of the protein aggregates on time for mAAT aggregation at 60°C registered at various protein concentrations: 0.05 (*1*), 0.1 (*2*), 0.2 (*3*) and 0.4 (*4*) mg/ml. *Solid curves* were calculated from Eq. (2). The *upper scale* shows the portion of the denatured protein (γ_{den}) calculated from Eq. (4) with $k_{den} = 5.1 \times 10^{-4}$ min^{-1}

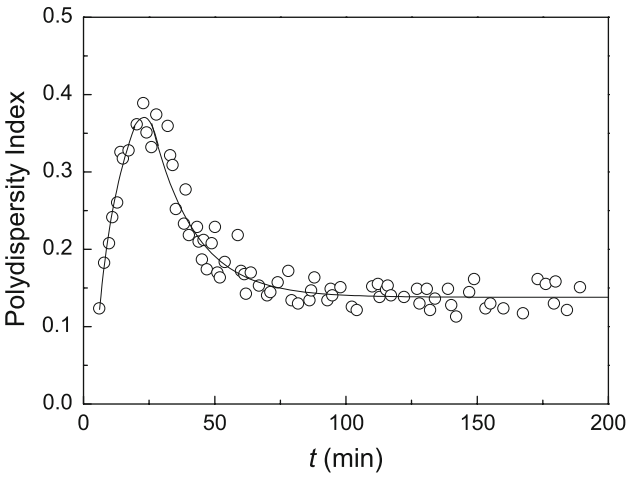

Fig. 3 The change in the polydispersity index PI in time for aggregation of mAAT (0.2 mg/ml) at 60°C

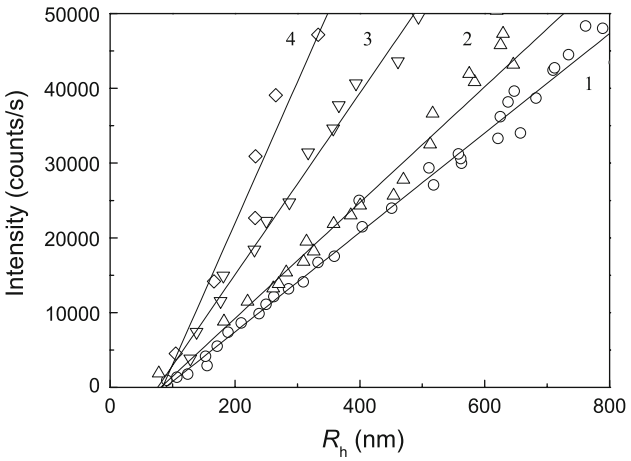

Fig. 4 The relationship between the light scattering intensity and hydrodynamic radius of the protein aggregates for aggregation of mAAT (0.2 mg/ml) at 60°C. The protein concentrations were as follows: 0.05 (*1*), 0.1 (*2*), 0.2 (*3*) and 0.4 (*4*) mg/ml

shows the dependences of the protein aggregates hydrodynamic radius on time for mAAT aggregation at 60°C. Analogous dependences were obtained at other temperatures (55 and 57.5°C). As it can be seen, the aggregation process is accompanied by monotonous increase in the R_h values up to the values in the region of ~2000 nm, where precipitation of the protein aggregates occurs.

To characterize the breadth of the protein aggregates distribution by size, the polydispersity index PI was calculated. Figure 3 shows a typical pattern of the change in the polydispersity index in time for aggregation of mAAT (0.2 mg/ml) at 60°C. The initial increase in the PI value in the course of aggregation changes into the exponential decay at $t > 25$ min. The limiting value of PI at $t \to \infty$ was found to be 0.14 ± 0.01.

Before proceeding to an analysis of the shape of the dependences of R_h on time shown in Fig. 2, we constructed the light scattering intensity versus hydrodynamic radius plots. Figure 4 shows such plots obtained for the aggregation of mAAT at 60°C. The initial parts of the dependences of the light scattering intensity on R_h are linear:

$$I = I_2\left(R_h - R_{h,0}\right), \tag{5}$$

where $R_{h,0}$ is the hydrodynamic radius of the start aggregates and I_2 is a constant. $R_{h,0}$ corresponds to the length cut off on the abscissa axis by the linear dependence of I on R_h. The values of parameters of I_2 and $R_{h,0}$ calculated at various temperatures and various mAAT concentrations are given in Table 1. As evident from the table, the variation of temperature or protein concentration does not result in appreciable changes in the $R_{h,0}$ value. The average value of the hydrodynamic radius of the start aggregates was found to be 78.5 ± 1.0 nm. It should be noted that under the used conditions only the protein aggregates are registered by DLS. To estimate the size of the original mAAT molecule, we carried out the DLS measurements using mAAT solution at a concentration of 4.6 mg/ml. The hydrodynamic radius of native mAAT at 20°C was found to be 4.13 ± 0.18 nm.

The fact that the size of the start aggregates remains unchanged with variation of the protein concentration is not surprising. Such a situation was observed by us earlier in the case of thermal aggregation of β_L-crystallin (Khanova et al. 2005), glyceraldehyde-3-phosphate dehydrogenase and glycogen phosphorylase *b* from rabbit skeletal muscle

Table 1 Parameters of Eqs. (1), (2) and (5) used for description of the kinetics of thermal aggregation of mAAT (10 mM Na-phosphate buffer, pH 7.5)

Temperature (°C)	Concentration of mAAT (mg/ml)	$I_2 \times 10^{-3}$ [(counts/s)/nm]	$R_{h,0}$ (nm)	$(1/t_{2R}) \times 10^2$ (min^{-1})	t^* (min)	R_h^* (nm)	d_f
55	0.05	0.94 ± 0.02	79.2 ± 0.9	5.2 ± 0.1	100	410	1.88 ± 0.02
55	0.1	2.0 (0.1)	76.2 ± 1.2	4.8 ± 0.1	100	430	1.86 ± 0.02
55	0.2	4.9 ± 0.2	71.3 ± 1.4	8.1 ± 0.2	60	395	1.85 ± 0.02
55	0.4	7.9 ± 0.2	72.6 ± 1.3	11.2 ± 0.3	30	340	1.84 ± 0.02
57.5	0.05	4.9 ± 0.2	85.9 ± 1.4	9.8 ± 0.2	55	480	1.76 ± 0.02
57.5	0.1	6.7 ± 0.1	81.9 ± 1.0	8.9 ± 0.2	50	470	1.81 ± 0.02
57.5	0.2	11.1 ± 0.1	84.4 ± 0.6	13.3 ± 0.3	40	500	1.87 ± 0.02
57.5	0.4	17.9 ± 0.5	72.6 ± 1.1	12.7 ± 0.2	40	430	1.80 ± 0.02
60	0.05	3.1 ± 0.1	76.9 ± 0.8	20 ± 1	15	310	1.84 ± 0.02
60	0.1	3.7 ± 0.2	81.0 ± 1.4	24 ± 1	15	360	1.84 ± 0.02
60	0.2	5.4 ± 0.2	75.9 ± 0.7	32 ± 2	15	475	1.80 ±0.02
60	0.4	9.7 ± 0.2	83.8 ± 0.9	50 ± 3	15	650	1.81 ± 0.02

(Markossian et al. 2006a, 2006b; Golub et al. 2007) and tobacco mosaic virus coat protein (Panyukov et al. 2007). Previously, we documented well that formation of the start aggregates proceeds on the all or none principle (Golub et al. 2007). It is evident that formation of the start aggregates resembles formation of micelles of surfactants.

With the knowledge of the $R_{h,0}$ values, we analyzed the initial parts of the dependences of R_h on time using Eq. (2). The values of the parameter $1/t_{2R}$ characterizing the rate of aggregation are given in Table 1. The $1/t_{2R}$ value increases with increasing temperature or protein concentration.

Above a certain value of time ($t > t^*$), the dependences of R_h on time follow the power law (Eq. 1) with parameter d_f close to 1.8 (the values of t^*, R_h^* and d_f are given in Table 1). Such a character of the dependences of R_h on time shows that thermal aggregation of mAAT proceeds in the diffusion-limited cluster–cluster regime as is the case with thermal aggregation of other proteins (Khanova et al. 2005; Markossian et al. 2006a, 2006b; Meremyanin et al. 2008).

The comparison of curve 3 in Fig. 2, on the one hand, and Fig. 3, on the other hand, shows that the ascending branch of the dependence of the polydispersity index PI on time corresponds to the linear part of the dependence of R_h on time ($t < t^* = 15$ min). As for the descending branch of the above-mentioned dependence, it corresponds to the part of the dependence of R_h on time that follows the power law ($t > t^* = 15$ min). The complex character of the dependence of PI on time indicates that different physical processes take place at $t < t^*$ and $t > t^*$. The region $t < t^*$ is the time interval where the start aggregates come into being, their emergence proceeding on the all or none principle (Golub et al. 2007). Simultaneously with emergence of the start aggregates, they start to stick. It should be noted that the denaturation process continues and new denatured protein molecules and consequently new start aggregates are formed. The appearance of new primary clusters in addition to the previously formed clusters results in the broadening of the distribution of aggregates by size and consequently in the increase in the PI value. The region $t > t^*$ is the time interval where the main process is the sticking of particles existing in the system. Since the sticking of the particles proceeds in the DLCA regime, the distribution of particles by size becomes rather narrow [see for discussion (Weitz et al. 1985)]. The PI value falls to 0.14 ± 0.01.

Effect of α-crystallin on thermal aggregation of mAAT

The suppression of mAAT aggregation by α-crystallin was studied by DLS. Figure 5 demonstrates the decrease in the

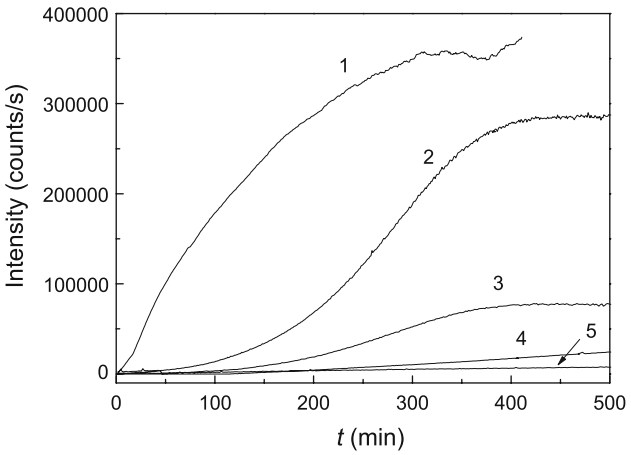

Fig. 5 Suppression of mAAT aggregation by α-crystallin. The dependences of the light scattering intensity on time for aggregation of mAAT (0.2 mg/ml or 4.4 μM calculated on monomer) at 60°C. The concentrations of α-crystallin were as follows: 0 (*1*), 0.1 (*2*), 0.15 (*3*), 0.2 (*4*) and 0.4 (*5*) mg/ml or 0 (*1*), 5 (*2*), 7.5 (*3*), 10 (*4*) and 20 (*5*) μM (calculated on monomer)

increment of the light scattering intensity accompanying the process of aggregation of mAAT (0.2 mg/ml) in the presence of α-crystallin. Almost complete suppression of mAAT aggregation was observed when the concentration of α-crystallin was 0.4 mg/ml (curve 5 in Fig. 5).

The dependences of the hydrodynamic radius of the protein aggregates on time are of considerable importance in the understanding of the mechanism of the protective action of α-crystallin. Figure 6 shows such dependences for aggregation of mAAT (0.2 mg/ml) at 60°C in the presence of various concentrations of α-crystallin. As it can be seen, at rather high times the splitting of the aggregate population into two components takes place. The point in time at which the unimodal distribution of the aggregates by size changes into the bimodal distribution was designated as t_{crit} (Table 2). It should be noted that such a splitting of the aggregate population into two components is typical of heat-induced protein aggregation in the presence of α-crystallin (Khanova et al. 2005; Markossian et al. 2006b).

The distinctive property of the dependences of R_h on time obtained for mAAT aggregation in the presence of α-crystallin is that the initial parts of these dependences are concave and follow the exponential law. The following equation for the exponential law was proposed in our previous papers (Khanova et al. 2007; Meremyanin et al. 2007, 2008.

$$R_h = R_{h,0}\exp[(\ln 2)(t - t_0)/t_{2R}], \quad (6)$$

where $R_{h,0}$ is the hydrodynamic radius of the initial particles participating in the aggregation process, t_0 is the lag period for the aggregation process and t_{2R} is the time interval over which the R_h value of aggregates is doubled.

To determine parameter $R_{h,0}$, the light scattering intensity versus the hydrodynamic radius plots were used. As can be seen from Fig. 7, the initial parts of the dependences of I on R_h are linear and the length cut off on the abscissa axis by the linear dependence of I on R_h gives the $R_{h,0}$ value. The dependence of I on R_h obtained for mAAT aggregation in the absence of α-crystallin is also shown in Fig. 7 (curve 1). The hydrodynamic radius of the initial particles ($R_{h,0}$) participating in the aggregation process greatly decreases in the presence of α-crystallin. For the used concentrations of α-crystallin (0.1–0.4 mg/ml) the $R_{h,0}$ values are practically identical and the average value the $R_{h,0}$ was found to be 17.7 ± 1.3 nm (Table 2). It should be noted that this $R_{h,0}$ value exceeds the R_h value for α-crystallin under non-aggregating conditions (R_h = 11.0 ± 0.1 nm; Khanova et al. 2007).

With the knowledge of $R_{h,0}$ value, we analyzed the dependences of the hydrodynamic radius of the protein aggregates on time for mAAT aggregation in the presence of α-crystallin. As it can be seen from the insets in Fig. 6a–c, the

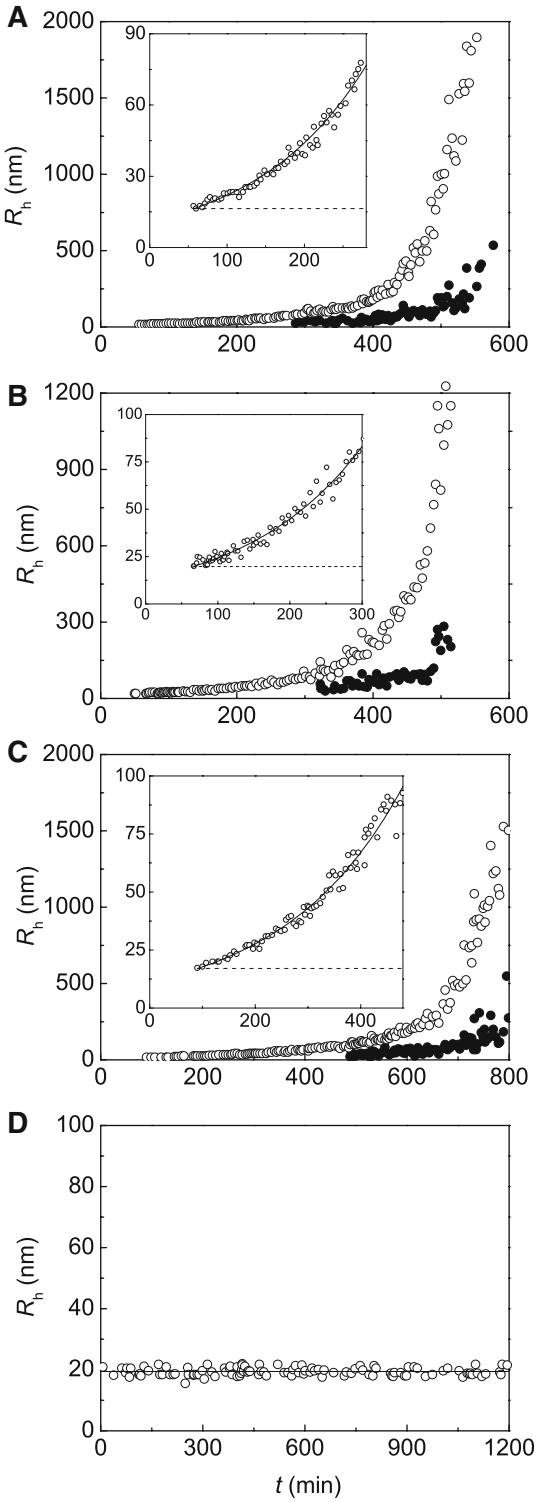

Fig. 6 Dependences of hydrodynamic radius (R_h) of the protein aggregates on time for aggregation of mAAT (0.2 mg/ml) at 60°C in the presence of α-crystallin. The concentrations of α-crystallin were as follows: 0.1 (**a**), 0.15 (**b**), 0.2 (**c**) and 0.4 (**d**) mg/ml. Insets in (**a**–**c**) show the initial parts of the dependences of R_h on time. *Solid curves* are calculated from Eq. (6). The *dotted horizontal lines* correspond to the $R_{h,0}$ values

Table 2 Parameters of Eqs. (5) and (6) used for description of the kinetics of thermal aggregation of mAAT (0.2 mg/ml) at 60°C in the presence of α-crystallin

Concentration of α-crystallin (mg/ml)	$I_2 \times 10^{-3}$ [(counts/s)/nm]	$R_{h,0}$ (nm)	t_0 (min)	$(1/t_{2R}) \times 10^2$ (min^{-1})	t_{crit} (min)
0.1	42.6 ± 0.4	16.4 ± 0.1	57.5 ± 1.1	1.00 ± 0.02	290
0.15	15.5 ± 0.3	19.7 ± 0.2	66.1 ± 1.4	0.89 ± 0.02	320
0.2	6.5 ± 0.1	17.1 ± 0.2	93.0 ± 4.0	0.07 ± 0.03	490
0.4	–	19.4 ± 0.1	–	–	–

initial parts of the dependences of R_h on time obtained in the presence of α-crystallin at concentrations 0.1, 0.15 and 0.2 mg/ml are satisfactorily described by Eq. (6). Parameters t_0 and $1/t_{2R}$ obtained by this procedure are given in Table 2. The t_0 value characterizing the duration of the lag period of the aggregation process increased with increasing the concentration of α-crystallin. The values of $1/t_{2R}$ parameter measured at various concentrations of α-crystallin testify that the rate of aggregation decreases in the presence of α-crystallin.

It should be noted that at rather high concentrations of α-crystallin (0.4 mg/ml) the size of the particles registered in the system remained constant ($R_h = 19.4 \pm 0.1$ nm) over at least 1,200 min (Fig. 6d).

The exponential character of the dependence of the hydrodynamic radius of the protein aggregates on time for aggregation of mAAT in the presence of α-crystallin means that the aggregation process develops in the RLCA regime. Such a transition of the DLCA regime into the RLCA regime in the presence of α-crystallin was also observed for thermal aggregation of calf eye lens β_L-crystallin (Khanova et al. 2005), glyceraldehyde-3-phosphate dehydrogenase (Markossian et al. 2006b) and glycogen phosphorylase *b* (Meremyanin et al. 2008) from rabbit skeletal muscle. Thus, results obtained in the present work support our idea

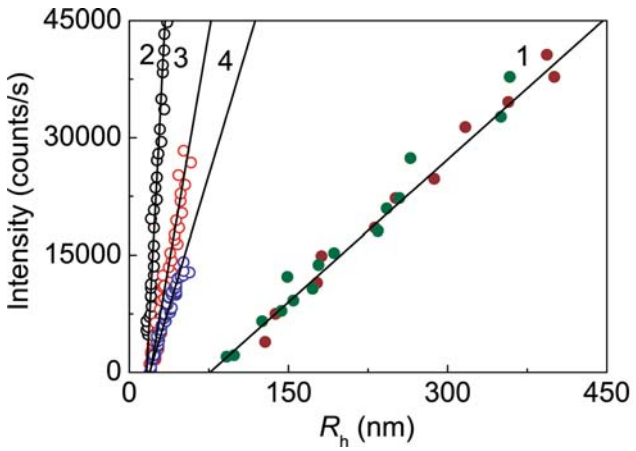

Fig. 7 The relationship between the light scattering intensity and hydrodynamic radius of the protein aggregates for aggregation of mAAT (0.2 mg/ml) at 60°C in the presence of the following concentrations of α-crystallin: 0 (*1*; the results of two experiments are shown), 0.1 (*2*), 0.15 (*3*) and 0.2 (*4*) mg/ml

(Khanova et al. 2005; Markossian et al. 2006b; Meremyanin et al. 2008) that the protective action of α-crystallin is due to the diminishing of the sticking probability for the colliding particles formed in the process of aggregation.

The results of the investigation of the kinetics of thermal aggregation of mAAT by DLS support the previously proposed mechanism of the amorphous protein aggregate formation at elevated temperatures (Golub et al. 2007; Khanova et al. 2005; Markossian et al. 2006a; Panyukov et al. 2007). The initial stage of aggregation is the stage of formation of the start aggregates (the primary clusters), the hydrodynamic radius of the latter being tens of nanometers. The theories of nucleation-dependent aggregation suggest that the growth of protein aggregates proceeds as a result of an attachment of the denatured protein molecule to a growing aggregate (Kodaka 2004a, 2004b; Kopito 2000; Kurganov 2002a, 2002b; Kurganov et al. 2002). These theories predict that the size of the protein aggregates should reach the limiting value when all denatured protein passes into an aggregated form. The fact that enhancement of the hydrodynamic radius of the protein aggregates continues up to values of 2,000–3,000 nm, at which precipitation of aggregates occurs, conflicts with the mechanism of nucleation-dependent aggregation. It is more realistic to suppose that the main pathway of the growth of the protein aggregates is the sticking of the start aggregates and aggregates of higher order. The application of the approaches elaborated to the study of colloid aggregation (Lin et al. 1990; Weitz et al. 1984, 1985) has allowed us to conclude that the sticking of the protein aggregates proceeds in the DLCA regime. The results obtained in the present work together with the previous data (Khanova et al. 2005; Markossian et al. 2006b; Meremyanin et al. 2007, 2008) have shown that the anti-aggregating effect of α-crystallin, one of the representatives of the family of small heat-shock proteins, is due to transition of the aggregation process into the RLCA regime where the sticking probability for the colliding particles becomes less than unity, as well as to diminution of the size of the initial particles participating in the aggregation process.

Acknowledgments This study was funded by the Russian Foundation for Basic Research (grants 08-04-00666-a and 06-04-39008_a), the Program "Molecular and Cell Biology" of the Presidium of the Russian Academy of Sciences and the State Scientific Program of the Republic of Belarus "Biological Engineering and Biosafety".

References

Abgar S, Vanhoudt J, Aerts T, Clauwaert J (2001) Study of the chaperoning mechanism of bovine lens alpha-crystallin, a member of the alpha small heat shock superfamily. Biophys J 80:1986–1995

Andreasi Bassi F, Arcovito G, De Spirito M, Mordente A, Martorana GE (1995) Self-similarity properties of alpha-crystallin supramolecular aggregates. Biophys J 69:2720–2727

Azzariti A, Vacca RA, Giannattasio S, Merafina RS, Marra E, Doonan S (1998) Kinetic properties and thermal stabilities of mutant forms of mitochondrial aspartate aminotransferase. Biochim Biophys Acta 1386:29–38

Ball RC, Weitz DA, Witten TA, Leyvraz F (1987) Universal kinetics in reaction-limited aggregation. Phys Rev Lett 58:274–277. doi:10.1103/PhysRevLett.58.274

Barra D, Bossa F, Doonan S, Fahmy HM, Martini F, Hughes GJ (1976) Large-scale purification and some properties of the mitochondrial aspartate aminotransferase from pig heart. Eur J Biochem 64:519–526. doi:10.1111/j.1432-1033.1976.tb10331.x

Berka M, Rice JA (2005) Relation between aggregation kinetics and the structure of kaolinite aggregates. Langmuir 21:1223–1229. doi:10.1021/la0478853

Bhattacharyya J, Santhoshkumar P, Sharma KK (2003) A peptide sequence -YSGVCHTDLHAWHGDWPLPVK- [40–60] in yeast alcohol dehydrogenase prevents the aggregation of denatured substrate proteins. Biochem Biophys Res Commun 307:1–7. doi:10.1016/S0006-291X(03)01116-1

Boyd JW (1961) The intracellular distribution, latency and electrophoretic mobility of L-glutamate-oxaloacetate transaminase from rat liver. Biochem J 81:434–441

Burgio MR, Kim CJ, Dow CC, Koretz JF (2000) Correlation between the chaperone-like activity and aggregate size of alpha-crystallin with increasing temperature. Biochem Biophys Res Commun 268:426–432. doi:10.1006/bbrc.1999.2036

Chiou SH, Azari P, Himmel ME, Squire PG (1979) Isolation and physical characterization of bovine lens crystallins. Int J Pept Protein Res 13:409–417

Dobson CM (1999) Protein misfolding, evolution and disease. Trends Biochem Sci 24:329–332. doi:10.1016/S0968-0004(99)01445-0

Fink AL (1998) Protein aggregation: folding aggregates, inclusion bodies and amyloid. Fold Des 3:R9–R23. doi:10.1016/S1359-0278(98)00002-9

Ford GC, Eichele G, Jansonius JN (1980) Three-dimensional structure of a pyridoxal-phosphate-dependent enzyme, mitochondrial aspartate aminotransferase. Proc Natl Acad Sci USA 77:2559–2563. doi:10.1073/pnas.77.5.2559

Golub N, Meremyanin A, Markossian K, Eronina T, Chebotareva N, Asryants R, Muronets V, Kurganov B (2007) Evidence for the formation of start aggregates as an initial stage of protein aggregation. FEBS Lett 581:4223–4227. doi:10.1016/j.febslet.2007.07.066

Golub NV, Markossian KA, Kasilovich NV, Sholukh MV, Orlov VN, Kurganov BI (2008) Thermal inactivation, denaturation and aggregation of mitochondrial aspartate aminotransferase. Biophys Chem 135:125–131. doi:10.1016/j.bpc.2008.04.001

Groenen PJ, Merck KB, de Jong WW, Bloemendal H (1994) Structure and modifications of the junior chaperone alpha-crystallin. From lens transparency to molecular pathology. Eur J Biochem 225:1–19. doi:10.1111/j.1432-1033.1994.00001.x

Horwitz J (1992) Alpha-crystallin can function as a molecular chaperone. Proc Natl Acad Sci USA 89:10449–10453. doi:10.1073/pnas.89.21.10449

Horwitz J (1993) Proctor lecture: the function of alpha-crystallin. Invest Ophthalmol Vis Sci 34:10–22

Horwitz J (2003) Alpha-crystallin. Exp Eye Res 76:145–153. doi:10.1016/S0014-4835(02)00278-6

International standard ISO 13321:1996(E) (1996) Particle size analysis-photon correlation spectroscopy. International Organization for Standartization, Geneva

Jaenicke R (1995) Folding and association versus misfolding and aggregation of proteins. Philos Trans R Soc Lond B Biol Sci 348:97–105. doi:10.1098/rstb.1995.0050

Jaenicke R (1998) Protein self-organization in vitro and in vivo: partitioning between physical biochemistry and cell biology. Biol Chem 379:237–243

Khanova HA, Markossian KA, Kurganov BI, Samoilov AM, Kleimenov SY, Levitsky DI, Yudin IK, Timofeeva AC, Muranov KO, Ostrovsky MA (2005) Mechanism of chaperone-like activity: suppression of thermal aggregation of beta L-crystallin by alpha-crystallin. Biochemistry 44:15480–15487. doi:10.1021/bi051175u

Khanova HA, Markossian KA, Kleimenov SY, Levitsky DI, Chebotareva NA, Golub NV, Asryants RA, Muronetz VI, Saso L, Yudin IK, Muranov KO, Ostrovsky MA, Kurganov BI (2007) Effect of alpha-crystallin on thermal denaturation and aggregation of rabbit skeletal muscle glyceraldehyde-3-phosphate dehydrogenase. Biophys Chem 125:521–531. doi:10.1016/j.bpc.2006.11.002

Kodaka M (2004a) Interpretation of concentration-dependence in aggregation kinetics. Biophys Chem 109:325–332. doi:10.1016/j.bpc.2003.12.003

Kodaka M (2004b) Requirements for generating sigmoidal time-course aggregation in nucleation-dependent polymerization model. Biophys Chem 107:243–253. doi:10.1016/j.bpc.2003.09.013

Kopito RR (2000) Aggresomes, inclusion bodies and protein aggregation. Trends Cell Biol 10:524–530. doi:10.1016/S0962-8924(00)01852-3

Krivandin AV, Muranov KO, Ostrovskii MA (2004) Studies of α- and β_L-crystallin complex formation in solution at 60°C. Mol Biol (Mosc) 38:532–546

Kurganov BI (2002a) Kinetics of protein aggregation. Quantitative estimation of the chaperone-like activity in test-systems based on suppression of protein aggregation. Biochemistry (Mosc) 67:409–422. doi:10.1023/A:1015277805345

Kurganov BI (2002b) Estimation of the activity of molecular chaperones in test-systems based on suppression of protein aggregation. Usp Biol Khim Mosc 42:89–138

Kurganov BI, Rafikova ER, Dobrov EN (2002) Kinetics of thermal aggregation of tobacco mosaic virus coat protein. Biochemistry (Mosc) 67:631–640

Lawton JM, Doonan S (1998) Thermal inactivation and chaperonin-mediated renaturation of mitochondrial aspartate aminotransferase. Biochem J 334(Pt 1):219–224

Le Bon C, Nicolai T, Durand D (1999) Kinetics of aggregation and gelation of globular proteins after heat-induced denaturation. Macromolecules 32:6120–6127. doi:10.1021/ma9905775

Lin MY, Lindsay HM, Weitz DA, Ball RC, Klein R, Meakin P (1989) Universality of fractal aggregates as probed by light scattering. Proc R Soc Lond A Math Phys Sci 423:71–87. doi:10.1098/rspa.1989.0042

Markossian KA, Kurganov BI (2004) Protein folding, misfolding, and aggregation: formation of inclusion bodies and aggresomes. Biochemistry (Mosc) 69:971–984. doi:10.1023/B:BIRY.0000043539.07961.4c

Markossian KA, Khanova HA, Kleimenov SY, Levitsky DI, Chebotareva NA, Asryants RA, Muronetz VI, Saso L, Yudin IK, Kurganov BI (2006a) Mechanism of thermal aggregation of rabbit muscle glyceraldehyde-3-phosphate dehydrogenase. Biochemistry 45:13375–13384. doi:10.1021/bi0610707

Markossian KA, Kurganov BI, Levitsky DI, Khanova HA, Chebotareva NA, Samoilov AM, Eronina TB, Fedurkina NV, Mitskevich LG, Merem'yanin AV, Kleymenov SY, Makeeva VF, Muronets VI, Naletova IN, Shalova IN, Asryants RA, Schmalhausen EV, Saso L, Panyukov YV, Dobrov EN, Yudin IK, Timofeeva AC, Muranov KO, Ostrovsky MA (2006b) Mechanisms of chaperone-like activity. In: Obalinsky TR (ed) Protein folding: new research. Nova Science, New York, pp 89–171

Markossian KA, Golub NV, Khanova HA, Levitsky DI, Poliansky NB, Muranov KO, Kurganov BI (2008) Mechanism of thermal aggregation of yeast alcohol dehydrogenase. I. Role of intramolecular chaperone. Biochim Biophys Acta 1784(9):1286–1293

Meremyanin AV, Eronina TB, Chebotareva NA, Kleimenov SY, Yudin IK, Muranov KO, Ostrovsky MA, Kurganov BI (2007) Effect of alpha-crystallin on thermal aggregation of glycogen phosphorylase b from rabbit skeletal muscle. Biochemistry (Mosc) 72:518–528. doi:10.1134/S0006297907050082

Meremyanin AV, Eronina TB, Chebotareva NA, Kurganov BI (2008) Kinetics of thermal aggregation of glycogen phosphorylase b from rabbit skeletal muscle: mechanism of protective action of alpha-crystallin. Biopolymers 89:124–134. doi:10.1002/bip.20872

Nicolai T, Durand D, Gimel JC (1994) Static structure factor of dilute solutions of polydisperse fractal aggregates. Phys Rev B Condens Matter 50:16357–16363. doi:10.1103/PhysRevB.50.16357

Panyukov Y, Yudin I, Drachev V, Dobrov E, Kurganov B (2007) The study of amorphous aggregation of tobacco mosaic virus coat protein by dynamic light scattering. Biophys Chem 127:9–18. doi:10.1016/j.bpc.2006.11.006

Pouzot M, Nicolai T, Durand D, Benyahia L (2004) Structure factor and elasticity of a heat-set globular protein gel. Macromolecules 37:614–620. doi:10.1021/ma035117x

Putilina T, Skouri-Panet F, Prat K, Lubsen NH, Tardieu A (2003) Subunit exchange demonstrates a differential chaperone activity of calf α-crystallin toward β_{LOW}- and individual γ-crystallins. J Biol Chem 278:13747–13756. doi:10.1074/jbc.M208157200

Twomey CM, Doonan S (1997) A comparative study of the thermal inactivation of cytosolic and mitochondrial aspartate aminotransferases. Biochim Biophys Acta 1342:37–44

Vanhoudt J, Aerts T, Abgar S, Clauwaert J (1997) Quaternary structure and interaction parameters of bovine α-crystallin: influence of isolation conditions. Prog Colloid Polym Sci 107:88–93. doi:10.1007/BFb0118019

Wang JK, Spector A (1994) The chaperone activity of bovine α-crystallin. Interaction with other lens crystallins in native and denatured states. J Biol Chem 269:13601–13608

Weitz DA, Huang JS, Lin MY, Sung J (1984) Dynamics of diffusion-limited kinetic aggregation. Phys Rev Lett 53:1657–1660. doi:10.1103/PhysRevLett.53.1657

Weitz DA, Huang JS, Lin MY, Sung J (1985) Limits of the fractal dimension for irreversible kinetic aggregation of gold colloids. Phys Rev Lett 54:1416–1419. doi:10.1103/PhysRevLett.54.1416

Xu S, Wu D, Arnsdorf M, Johnson R, Getz GS, Cabana VG (2005) Chemical colloids versus biological colloids: a comparative study for the elucidation of the mechanism of protein fiber formation. Biochemistry 44:5381–5389. doi:10.1021/bi0474719